

Synthesis of Carbon/Sulfur Nanolaminates by Electrochemical Extraction of Titanium from Ti_2SC **

Meng-Qiang Zhao, Morgane Sedran, Zheng Ling, Maria R. Lukatskaya, Olha Mashtalir, Michael Ghidui, Boris Dyatkin, Darin J. Tallman, Thierry Djenizian, Michel W. Barsoum, and Yury Gogotsi*

Abstract: Herein we electrochemically and selectively extract Ti from the MAX phase Ti_2SC to form carbon/sulfur (C/S) nanolaminates at room temperature. The products are composed of multi-layers of C/S flakes, with predominantly amorphous and some graphene-like structures. Covalent bonding between C and S is observed in the nanolaminates, which render the latter promising candidates as electrode materials for Li-S batteries. We also show that it is possible to extract Ti from other MAX phases, such as Ti_3AlC_2 , Ti_3SnC_2 , and Ti_2GeC , suggesting that electrochemical etching can be a powerful method to selectively extract the “M” elements from the MAX phases, to produce “AX” layered structures, that cannot be made otherwise. The latter hold promise for a variety of applications, such as energy storage, catalysis, etc.

In the past decade, two-dimensional (2D) materials including graphene, metal oxides/hydroxides, boron nitride (BN), dichalcogenides, and transition metal carbides/carbonitrides (MXenes), have attracted much attention.^[1] In most cases, 2D materials are produced by exfoliation or delamination of van der Waals solids, such as graphite and MoS_2 .^[1f,2] The direct reaction between different elements, or compounds, is also a general synthesis approach for the formation of 2D

materials, such as the chemical vapor deposition of graphene from hydrocarbons^[3] and the co-precipitation of metal hydroxides/oxides.^[4] Recently, there has also been great interest in selective extraction processes to produce 2D materials due to its ability to achieve well-controlled morphologies and structures, and even generate new materials that cannot be produced by other methods.^[1e,5]

One of the best known, and most studied selective extraction processes is the synthesis of carbide-derived carbons (CDCs) with high specific surface areas and tunable pore sizes, which involves the selective etching of metals from metal carbides.^[6] Many 2D materials have also been synthesized using this route. For instance, the epitaxial growth of graphene can be achieved by thermally extracting the Si atoms from SiC single crystals.^[5a] Another example is the formation of 2D transition metal oxides by the selective leaching out of alkali cations (K^+ , Cs^+ , etc.) from their layered three-dimensional (3D) salts.^[5b]

The MAX phases are a class of 3D layered, ternary carbides and nitrides that, stemming from their innate layered structures, are excellent precursors for 2D materials through selective extraction.^[1e,5c,6b,7] The MAX phases (Figure 1a, left) have a general formula of $\text{M}_{n+1}\text{AX}_n$, where M is an early transition metal (Ti, Nb, Mo, V, etc.), A is mostly IIIA and IVA group elements (Al, Si, Ge, etc.), X is carbon and/or

[*] Dr. M.-Q. Zhao, Z. Ling, M. R. Lukatskaya, O. Mashtalir, M. Ghidui, B. Dyatkin, D. J. Tallman, Prof. M. W. Barsoum, Prof. Y. Gogotsi
A. J. Drexel Nanomaterials Institute, and Materials Science and Engineering Department, Drexel University
3141 Chestnut Street, Philadelphia, PA 19104 (USA)
E-mail: gogotsi@drexel.edu

M. Sedran, Prof. T. Djenizian
Aix-Marseille University, MADIREL Laboratory
FR-13288 Marseille Cedex 9 (France)

Z. Ling
Carbon Research Laboratory, Liaoning Key Lab for Energy Materials and Chemical Engineering, State Key Lab of Fine Chemicals, Dalian University of Technology
Dalian 116024 (China)

[**] This work was supported by the U.S. Department of Energy, Office of Science, Basic Energy Sciences, under Award no. ER46473. Z.L. was supported by the Chinese Scholarship Council (CSC). M.S. and T.D. are grateful to the European agency and the Erasmus Mundus “Materials for Energy Storage and Conversion. XRD, SEM, TEM, and XPS investigations were performed at the Centralized Research Facilities (CRF) at Drexel University.

Supporting information for this article (MAX phase sample preparation procedures, electrochemical etching process, as well as the characterization techniques used and the electrochemical tests for Li-S batteries) is available on the WWW under <http://dx.doi.org/10.1002/anie.201500110>.

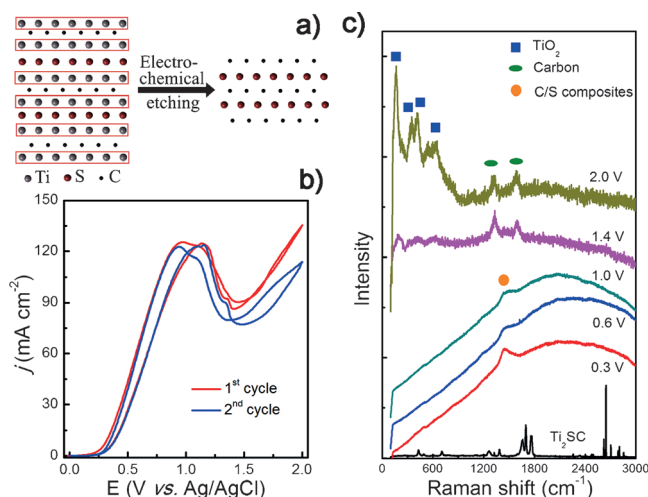


Figure 1. a) Schematic showing the selective extraction of Ti (M) from Ti_2SC (MAX) through electrochemical etching. b) CVs showing the etching process of Ti_2SC in a NH_4F aqueous electrolyte. c) Raman spectra of Ti_2SC before (bottom curve) and after etching at various potentials noted in figure with respect to Ag/AgCl.

nitrogen, and $n = 1-3$.^[8] In 2011, a family of new 2D materials, so called MXenes, were synthesized by selective extraction of “A” layers from the MAX phases.^[1d] About a dozen MXenes have been produced so far.^[1e,9] They offer an unusual combination of metallic conductivity and hydrophilicity, and exhibit excellent properties when used in Li-ion batteries, supercapacitors, or in polymer nanocomposites.^[9a,10] When both the M and A elements are extracted simultaneously, either by high-temperature Cl_2 etching^[11] or room-temperature electrochemical etching,^[7] CDCs with tunable pore sizes are produced.

Quite recently, an electrochemical, room temperature, etching method—that forgoes energy-intensive thermal treatments with reactive elements such as Cl_2 gas—to produce CDCs was developed.^[7,12] In our previous work, cyclic voltammograms (CVs) obtained for the MAX phases in different electrolytes showed the presence of two anodic steps/peaks,^[7] which suggested that the selective extraction of the “M” or “A” elements should be possible. The goal of this work was to explore the possibility to selectively extract the M element by electrochemically etching at lower potentials. The Ti_2SC MAX phase was selected for this study and an NH_4F aqueous solution was selected as the electrolyte.

Considering the relative electrochemical inertness of S, it is reasonable to anticipate that Ti would be easier to extract than S from Ti_2SC , resulting in carbon/sulfur (C/S) nanolaminates (Figure 1a). The CVs of a Ti_2SC sample etched in NH_4F aqueous solution between 0–2.0 V, with respect to Ag/AgCl, showed an obvious and reproducible peak around 1.0 V (Figure 1b). To understand the relationship between etching voltage and etching products, Ti_2SC was etched at 0.3, 0.6, 1.0, 1.4, and 2.0 V, and characterized. When the Raman spectrum of the sample etched at 0.3 V (second to bottom curve in Figure 1c) is compared to that of Ti_2SC (bottom curve in Figure 1c), it is clear that peaks for the latter disappear completely. Instead, a single mode, around 1440 cm^{-1} , most probably corresponding to carbyne polysulfide, was observed,^[13] indicating the selective extraction of Ti from the Ti_2SC and the formation of S–C bonds. Almost identical Raman spectra were observed for products etched at 0.6 and 1.0 V. At the highest etching potentials of 1.4 and 2.0 V, Raman peaks (top curve in Figure 1c) coinciding with those of CDC, were observed. More specifically, the presence of D ($\approx 1330\text{ cm}^{-1}$) and G ($\approx 1580\text{ cm}^{-1}$) peaks is obvious, indicating the extraction of both Ti and S.^[7] Raman peaks corresponding to TiO_2 were also observed at the highest voltages.

The Raman spectroscopy results were in good agreement with the scanning electron microscopy (SEM) and energy-dispersive spectroscopy (EDS) analysis (Figure S1; see the Supporting Information), in which, it was further confirmed that the Ti atoms were selectively extracted between 0.3 and 1.0 V (Figure S1a and b). The loss of S occurs at potentials $> 1.0\text{ V}$, accompanied by the formation of a TiO_2 passive layer (Figure S1c and d), which results in a significant drop of the current density in the CVs shown in Figure 1b. At potentials $> 1.4\text{ V}$, the increase in current density most probably corresponds to the active dissolution of a TiO_2 passive layer and/or electrolyte breakdown (Figure S1e and f). More

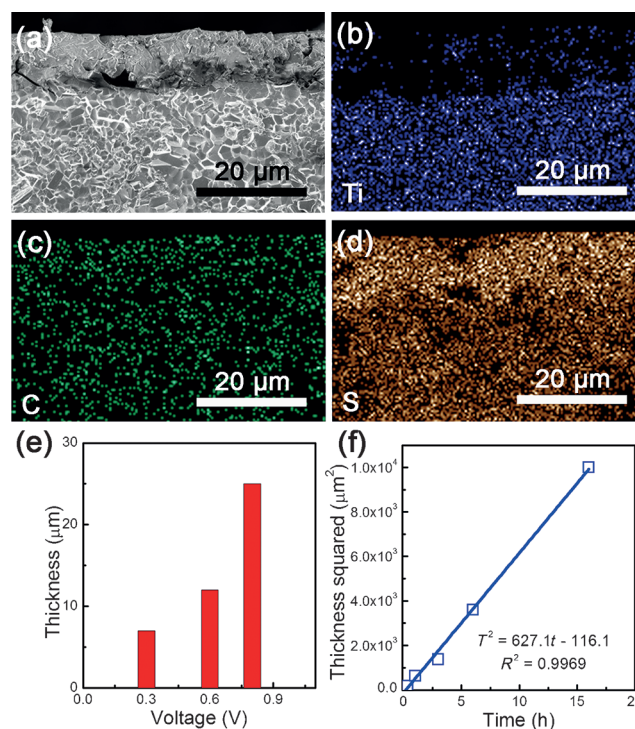


Figure 2. a) Cross-sectional SEM image of a Ti_2SC sample etched for 1 h at 0.6 V and b–d) corresponding EDS maps, indicating the selective extraction of Ti. e) Dependence of C/S layer thickness, after for 1 h, on etching voltage. f) C/S layer thickness vs. etching time at 0.8 V.

importantly, it was also demonstrated that the selective extraction of Ti was successfully achieved in other electrolytes, such as HCl and HF aqueous solutions (Figure S2 and S3).

EDS maps of Ti, C and S, on an etched and fractured surface (Figure 2a), shown, respectively, in Figures 2b–d, clearly show selective Ti extraction from the surface facing the electrolyte. Not surprisingly, the etching potential plays an important role in the etching rate. The thicknesses of the C/S layers after 1 h etching at 0.3, 0.6, and 0.8 V were ca. 7, 12, and 25 μm , respectively (Figure 2e). To quantify the etching kinetics, a series of experiments were carried out for different times, t , at 0.8 V. The resulting time dependencies of the thicknesses can be fit by the following parabolic expression: $T^2 = 627.1t - 116.1$, where T is the C/S layer thickness (Figure 2f), unlike the previous linear dependence observed when both “M” and “A” elements were extracted.^[7] It signifies that the process here is more, likely than not, diffusion controlled.

The C/S layers were easily detached from their Ti_2SC substrates (Figure S4) and pulverized. X-ray diffraction (XRD) patterns of the powders produced at a potential of 0.8 V are shown in Figure 3a. After etching (blue pattern in Figure 3a), the characteristic Ti_2SC peaks (bottom, red pattern in Figure 3a) totally disappear. Instead, TiO_2 peaks, denoted by solid squares in middle pattern in Figure 3a, are observed. High-resolution X-ray photoelectron spectroscopy (XPS) analysis of the Ti region further confirmed the absence of Ti–C bonds and the presence of Ti–O bonds instead

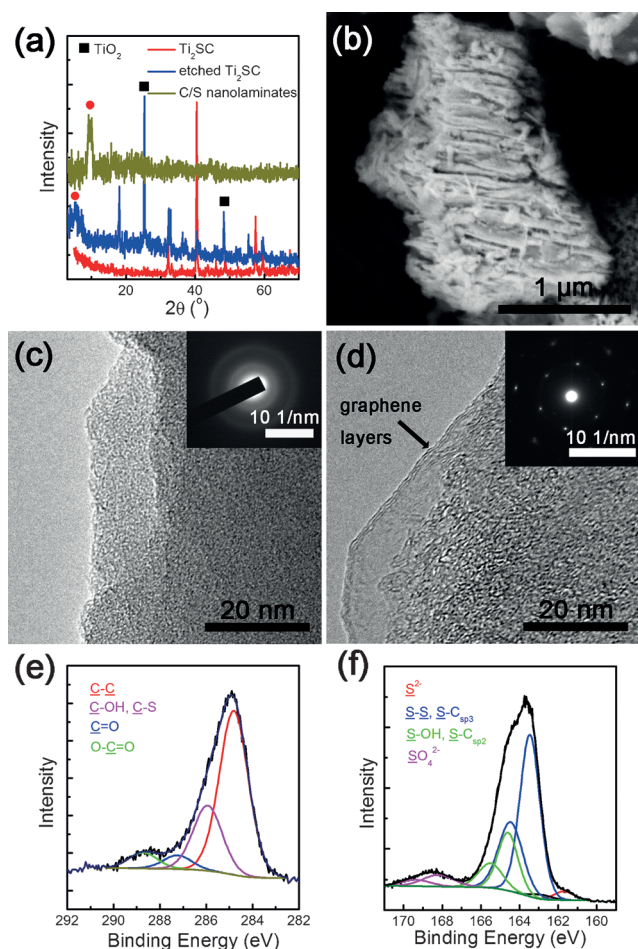


Figure 3. a) XRD patterns of Ti_2SC (red, bottom pattern), Ti_2SC etched for 3 h at 0.8 V before (blue, middle pattern) and after (green, top pattern) dissolving the TiO_2 particles in HF. Note disappearance of peaks denoted by solid squares in middle pattern that belong to TiO_2 . b) SEM image of a C/S particle. c,d) High-resolution TEM images of amorphous (c) and graphene-like (d) C/S flakes. Inserted are the corresponding SAED patterns. e,f) High-resolution XPS analysis of C1s (e) and S2p regions (f) in the C/S nanolaminates.

(Figure S5). The TiO_2 is presumed to come from the hydrolysis of the extracted Ti ions that are presumably trapped in the C/S framework.^[7] Removal of the oxide inclusions was accomplished by washing the etched samples with a 5 wt. % HF aqueous solution. The XRD pattern of the electrochemically-etched C/S powder (blue, middle pattern in Figure 3a) features a peak at $2\theta = 5.5^\circ$, which is most probably indicative of a layered structure with an inter-layer distance of 32.0 Å. After etching with dilute HF (green, top pattern in Figure 3a) only one peak—at 9.3° 2θ —remains. The corresponding c -LP is ca. 19.0 Å. This reduction in c -LP is probably due to the removal of interlayer TiO_2 during HF washing and intercalated H_2O during drying.

When a single C/S particle—several micrometers wide—was imaged in a SEM (Figure 3b) its layered nature was clear. High-resolution transmission electron microscopy (TEM) analysis reveals that the C/S nanolaminates are predominantly composed of amorphous C/S flakes (Figure 3c). However, it is important to note that some of the C/S flakes

($\approx 5\%$ based on statistical analysis of TEM images) exhibit a graphene-like structure, with a hexagonal selected area electron diffraction (SAED) pattern (Figure 3d). After HF-washing, the nanolaminates were quite pure (97 wt. %), with small amounts of residual TiO_2 (Figure S6a). Based on thermogravimetric (TGA), EDS, and XPS (Figures S6–S8) analysis, the S content in the C/S nanolaminates was determined to be 63 wt. %. Of that fraction, 52 wt. % exists as elemental S and the rest exist in the form of polysulfides, that is, C-S_x (Figure S6b). Analysis of high-resolution C1s and S2p XPS spectra regions suggests that the major constituents in the C/S nanolaminates are C–C, S–S, and C–S_x compounds, accompanied by O-containing functional groups bonded with either C or S atoms (Figure 3e,f).

Considering their unique layered structure, it is reasonable to assume that the C/S nanolaminates could be used as electrode materials for Li-S batteries.^[14] To test this idea, Li/S cells were fabricated and tested. Typical charge and discharge plateaus for Li-S batteries were observed in the galvanostatic profiles of the C/S nanolaminates within 1.0–3.0 V with respect to Li (Figure 4a), indicating a redox reaction between Li and S.^[15]

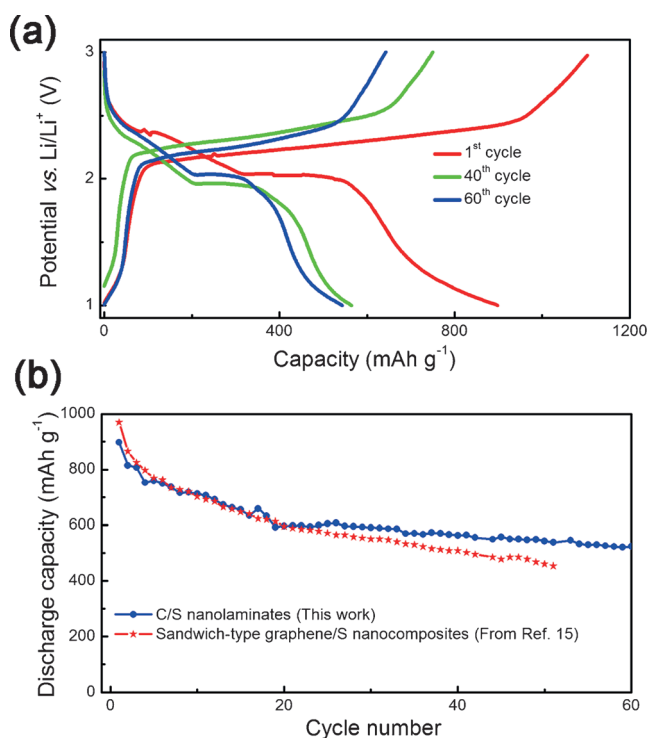


Figure 4. Electrochemical performance of C/S nanolaminates for Li-S batteries. a) Charge and discharge profiles. b) Cycling performance on discharging compared to sandwich-type graphene/S nanocomposite (Ref. [15]).

At a rate of 0.1 C, an initial discharge capacity of ca. 900 mAh g^{-1} was achieved (Figure 4b). It decreased to ca. 530 mAh g^{-1} after 60 cycles. A higher charge capacity, around 1200 mAh g^{-1} can be achieved at 0.1 C (Figure S9). Compared to sandwich-type graphene/S nanocomposites, prepared by incorporating S between graphene layers,^[15] the C/S nano-

laminates exhibited better cycling stability when tested under the same conditions. Indubitably, these characteristics, including cycling stability, coulombic efficiency, and rate performance, will be further improved through structural and particle size, etc. optimization. The performance can also be improved through optimization of the testing technique, including the cathode structure and electrolyte modulation, as well as the utilization of interlayers.^[16]

To demonstrate the general validity of our electrochemical etching process we applied it to other MAX phases, that is, Ti_3AlC_2 , Ti_3SnC_2 and Ti_2GeC . The results—summarized in Table 1 and Figure S10—clearly show that in all cases, the Ti

Table 1: EDS results showing the atomic ratios of the various elements in selected MAX phases after electrochemical etching.

	Ti_2SC	Ti_3AlC_2	Ti_3SnC_2	Ti_2GeC
Ti	0.1	0.1	0.02	0.3
"A" element (S, Al, Sn, Ge)	1.0	1.0	1.0	1.0
C	0.8	0.7	2.8	1.0
O	0.6	–	1.2	1.6

atoms were selectively extracted, and the corresponding "AX" structures, that is, Al/C, Sn/C and Ge/C nanostructures, were produced. Considering that >70 MAX phases are known to exist,^[8] it is not difficult to foresee that the "AX" structures represent a large new family of nanostructured materials, much of which will probably be 2D. The various "A" and "X" combinations known render the "AX" structures highly attractive for a number of potential applications, such as electrical energy storage, catalysis, etc. Synthesis of these new "AX" structures, as well as, their structural and property characterization certainly represent a very fertile area of research, with potentially huge payoffs.

In summary, we developed an electrochemical method to selectively extract Ti from Ti_2SC , resulting in C/S nanolaminates and TiO_2 . Dissolving the latter in dilute HF resulted in a high purity C/S nanolaminated amorphous flakes, with a c-LP of ca. 19.0 Å between them. A minority of these flakes were graphene-like. When tested as cathodes in Li/S batteries, their electrochemical performance was quite promising. Furthermore, we show that it is possible to electrochemically selectively extract Ti from a number of other MAX phases to create a new class of "AX" phases, most of which should be nanolayered.

Keywords: C/S nanolaminates · electrochemical etching · layered structures · MAX phase · selective extraction

How to cite: *Angew. Chem. Int. Ed.* **2015**, *54*, 4810–4814
Angew. Chem. **2015**, *127*, 4892–4896

- [1] a) K. S. Novoselov, D. Jiang, F. Schedin, T. J. Booth, V. V. Khotkevich, S. V. Morozov, A. K. Geim, *Proc. Natl. Acad. Sci. USA* **2005**, *102*, 10451–10453; b) V. Nicolosi, M. Chhowalla, M. G. Kanatzidis, M. S. Strano, J. N. Coleman, *Science* **2013**, *340*,

- 6139; c) R. Ma, T. Sasaki, *Adv. Mater.* **2010**, *22*, 5082–5104; d) M. Naguib, M. Kurtoglu, V. Presser, J. Lu, J. Niu, M. Heon, L. Hultman, Y. Gogotsi, M. W. Barsoum, *Adv. Mater.* **2011**, *23*, 4248–4253; e) M. Naguib, V. N. Mochalin, M. W. Barsoum, Y. Gogotsi, *Adv. Mater.* **2014**, *26*, 992–1005; f) S. Balendhran, S. Walia, H. Nili, J. Z. Ou, S. Zhuikov, R. B. Kaner, S. Sriram, M. Bhaskaran, K. Kalantar-zadeh, *Adv. Funct. Mater.* **2013**, *23*, 3952–3970; g) Y. Gao, D. Ma, G. Hu, P. Zhai, X. Bao, B. Zhu, B. Zhang, D. S. Su, *Angew. Chem. Int. Ed.* **2011**, *50*, 10236–10240; *Angew. Chem.* **2011**, *123*, 10419–10423.
- [2] C. N. R. Rao, A. K. Sood, K. S. Subrahmanyam, A. Govindaraj, *Angew. Chem. Int. Ed.* **2009**, *48*, 7752–7777; *Angew. Chem.* **2009**, *121*, 7890–7916.
- [3] a) X. Li, W. Cai, J. An, S. Kim, J. Nah, D. Yang, R. Piner, A. Velamakanni, I. Jung, E. Tutuc, S. K. Banerjee, L. Colombo, R. S. Ruoff, *Science* **2009**, *324*, 1312–1314; b) M.-Q. Zhao, Q. Zhang, J.-Q. Huang, G.-L. Tian, J.-Q. Nie, H.-J. Peng, F. Wei, *Nat. Commun.* **2014**, *5*, 3410.
- [4] a) Q. Wang, D. O'Hare, *Chem. Rev.* **2012**, *112*, 4124–4155; b) D. G. Evans, X. Duan, *Chem. Commun.* **2006**, 485–496.
- [5] a) K. V. Emtsev, A. Bostwick, K. Horn, J. Jobst, G. L. Kellogg, L. Ley, J. L. McChesney, T. Ohta, S. A. Reshanov, J. Rohrl, E. Rotenberg, A. K. Schmid, D. Waldmann, H. B. Weber, T. Seyller, *Nat. Mater.* **2009**, *8*, 203–207; b) M. Osada, T. Sasaki, *J. Mater. Chem.* **2009**, *19*, 2503–2511; c) M. Naguib, Y. Gogotsi, *Acc. Chem. Res.* **2015**, *48*, 128–135.
- [6] a) Y. Gogotsi, A. Nikitin, H. Ye, W. Zhou, J. E. Fischer, B. Yi, H. C. Foley, M. W. Barsoum, *Nat. Mater.* **2003**, *2*, 591–594; b) V. Presser, M. Heon, Y. Gogotsi, *Adv. Funct. Mater.* **2011**, *21*, 810–833.
- [7] M. R. Lukatskaya, J. Halim, B. Dyatkin, M. Naguib, Y. S. Buranova, M. W. Barsoum, Y. Gogotsi, *Angew. Chem. Int. Ed.* **2014**, *53*, 4877–4880; *Angew. Chem.* **2014**, *126*, 4977–4980.
- [8] M. W. Barsoum, *MAX Phases: Properties of Machinable Ternary Carbides and Nitrides*, Wiley, Hoboken, **2013**.
- [9] a) M. Naguib, J. Halim, J. Lu, K. M. Cook, L. Hultman, Y. Gogotsi, M. W. Barsoum, *J. Am. Chem. Soc.* **2013**, *135*, 15966–15969; b) M. Ghidui, M. Naguib, C. Shi, O. Mashtalir, L. M. Pan, B. Zhang, J. Yang, Y. Gogotsi, S. J. L. Billinge, M. W. Barsoum, *Chem. Commun.* **2014**, *50*, 9517–9520; c) M. Ghidui, M. R. Lukatskaya, M.-Q. Zhao, Y. Gogotsi, M. W. Barsoum, *Nature* **2014**, *516*, 78–81.
- [10] a) Q. Tang, Z. Zhou, P. Shen, *J. Am. Chem. Soc.* **2012**, *134*, 16909–16916; b) O. Mashtalir, M. Naguib, V. N. Mochalin, Y. Dall'Agnese, M. Heon, M. W. Barsoum, Y. Gogotsi, *Nat. Commun.* **2013**, *4*, 1716; c) M. R. Lukatskaya, O. Mashtalir, C. E. Ren, Y. Dall'Agnese, P. Rozier, P. L. Taberna, M. Naguib, P. Simon, M. W. Barsoum, Y. Gogotsi, *Science* **2013**, *341*, 1502–1505; d) Z. Ling, C. E. Ren, M.-Q. Zhao, J. Yang, J. M. Giammarco, J. Qiu, M. W. Barsoum, Y. Gogotsi, *Proc. Natl. Acad. Sci. USA* **2014**, *111*, 16676–16681; e) M.-Q. Zhao, C. E. Ren, Z. Ling, M. R. Lukatskaya, C. Zhang, K. L. Van Aken, M. W. Barsoum, Y. Gogotsi, *Adv. Mater.* **2015**, *27*, 339–345.
- [11] G. Yushin, E. N. Hoffman, M. W. Barsoum, Y. Gogotsi, C. A. Howell, S. R. Sandeman, G. J. Phillips, A. W. Lloyd, S. V. Mikhalevsky, *Biomaterials* **2006**, *27*, 5755–5762.
- [12] J. Senthilnathan, C.-C. Weng, W.-T. Tsai, Y. Gogotsi, M. Yoshimura, *Carbon* **2014**, *71*, 181–189.
- [13] B. Duan, W. Wang, A. Wang, K. Yuan, Z. Yu, H. Zhao, J. Qiu, Y. Yang, *J. Mater. Chem. A* **2013**, *1*, 13261–13267.
- [14] a) Y. X. Yin, S. Xin, Y. G. Guo, L. J. Wan, *Angew. Chem. Int. Ed.* **2013**, *52*, 13186–13200; *Angew. Chem.* **2013**, *125*, 13426–13441; b) P. G. Bruce, S. A. Freunberger, L. J. Hardwick, J. M. Tarascon, *Nat. Mater.* **2012**, *11*, 19–29; c) Q. Zhang, X.-b. Cheng, J.-q. Huang, H.-j. Peng, F. Wei, *Carbon* **2015**, *81*, 850.
- [15] Y. Cao, X. Li, I. A. Aksay, J. Lemmon, Z. Nie, Z. Yang, J. Liu, *Phys. Chem. Chem. Phys.* **2011**, *13*, 7660–7665.

- [16] a) L. Zhu, H.-J. Peng, J. Liang, J.-Q. Huang, C.-M. Chen, X. Guo, W. Zhu, P. Li, Q. Zhang, *Nano Energy* **2015**, *11*, 746–755; b) X.-B. Cheng, J.-Q. Huang, H.-J. Peng, J.-Q. Nie, X.-Y. Liu, Q. Zhang, F. Wei, *J. Power Sources* **2014**, 253, 263–268; c) H.-J. Peng, J.-Q. Huang, M.-Q. Zhao, Q. Zhang, X.-B. Cheng, X.-Y. Liu, W.-Z. Qian, F. Wei, *Adv. Funct. Mater.* **2014**, *24*, 2772–2781; d) L. Zhu, W. Zhu, X.-B. Cheng, J.-Q. Huang, H.-J. Peng, S.-H. Yang, Q. Zhang, *Carbon* **2014**, 75, 161–168; e) Y.-S. Su, A. Manthiram, *Nat. Commun.* **2012**, 3, 1166.

Received: January 7, 2015

Published online: February 25, 2015